ACS OMEGA

http://pubs.acs.org/journal/acsodf

Article

Reversible Absorption of Volatile Organic Compounds by Switchable-Hydrophilicity Solvents: A Case Study of Toluene with *N,N*-Dimethylcyclohexylamine

Yingjie Li, Haiyu Chang, Hui Yan, Senlin Tian,* and Philip G. Jessop*

Cite This: *ACS Omega* 2021, 6, 253−264

Read Online

ACCESS | Metrics & More | Article Recommendations | Supporting Information

ABSTRACT: Absorption is one of the most important treatment technologies for the removal of volatile organic compounds (VOCs) from tail gases, yet the separation of the absorbents and VOCs remains challenging because of concerns related to environmental impact and large energy requirements. Herein, we explored an absorption and desorption process using *N,N*-dimethylcyclohexylamine ($CyNMe_2$) as a representative switchable-hydrophilicity solvent (SHS) and toluene as a representative VOC. The results showed that in comparison to common absorbents, $CyNMe_2$ exhibits excellent toluene absorption performance. Desorption efficiencies of toluene from $CyNMe_2$ of up to 94% were achieved by bubbling CO_2 at 25 °C, and separation efficiencies of $CyNMe_2$ from water up to 90% were achieved by bubbling N_2 at 60 °C. Even after five absorption−desorption cycles, the toluene absorption capacity of $CyNMe_2$ was comparable with that of the fresh absorbent, suggesting that $CyNMe_2$ retains its absorption capacity. We demonstrate an innovative and reversible remediation strategy of VOCs based on SHSs, and the results indicate that SHSs can be used as an alternative to common absorbents for the removal of VOCs to reduce environmental pollution and energy consumption.

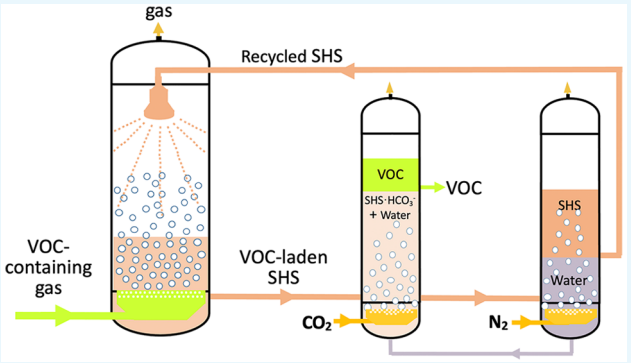

1. INTRODUCTION

Volatile organic compounds (VOCs) are important precursors of atmospheric secondary organic aerosols.[1,2] These compounds are emitted into the atmosphere from a wide range of industries, such as chemical, petrochemical, pharmaceutical, food processing, pulp and paper, color printing, and painting industries.[3] It was estimated that in China alone, approximately 10−20 Tg per year of VOCs are released into the atmosphere from anthropogenic sources, with 80% of the emission sources associated with coke and crude oil production and refining.[4] Generally, these industrial waste gases contain a high concentration of VOCs. For example, coke oven gas contains about 38 g/m^3 of benzoles (benzene 55−80%, toluene 11−22%, and xylene 2.5−6%; data from Kunming Coke Maker Factory, China). VOCs can enter the human body through the skin and respiratory system and cause temporary and permanent damage to the lungs, blood, liver, and other organ systems.[5] Therefore, advanced treatment technologies and methods to control atmospheric VOC pollution are urgently needed.

There are many available techniques to control the emission of VOCs, such as activated carbon adsorption, condensation, liquid absorption, membrane separation, incineration or thermal oxidation, catalytic oxidation, and biological treatments, each of which has disadvantages and limitations under different conditions.[6,7] Biological treatments, catalytic oxidation, incineration, and thermal oxidation techniques can easily destroy the structures of VOCs. In nondestructive technology, condensation is usually used in combination with compression, adsorption, and absorption. For membrane separation technology, membranes are costly. For adsorption, adsorbent regeneration is complex and can cause secondary pollution. Absorption, in which a contaminated gas is brought in contact with a liquid solvent, is one of the most frequently used technologies for the removal of VOCs from industrial waste gases because it is simple, easy to operate, and has reported removal efficiencies as high as 98%, especially for high-concentration VOCs,[8] and the absorbents can be reused.[9,10] A crucial aspect of this treatment method is the selection of a suitable absorbent: several common solvents have been used as absorbents for the removal of volatile contaminants, for example, washing oil (WO), vegetable oil,[11] mineral oil,[12] silicon oil,[13−15] diesel oil,[16] dimethyl sulfoxide,[17] polyglycols,[18]

Received: September 10, 2020
Accepted: December 11, 2020
Published: December 30, 2020

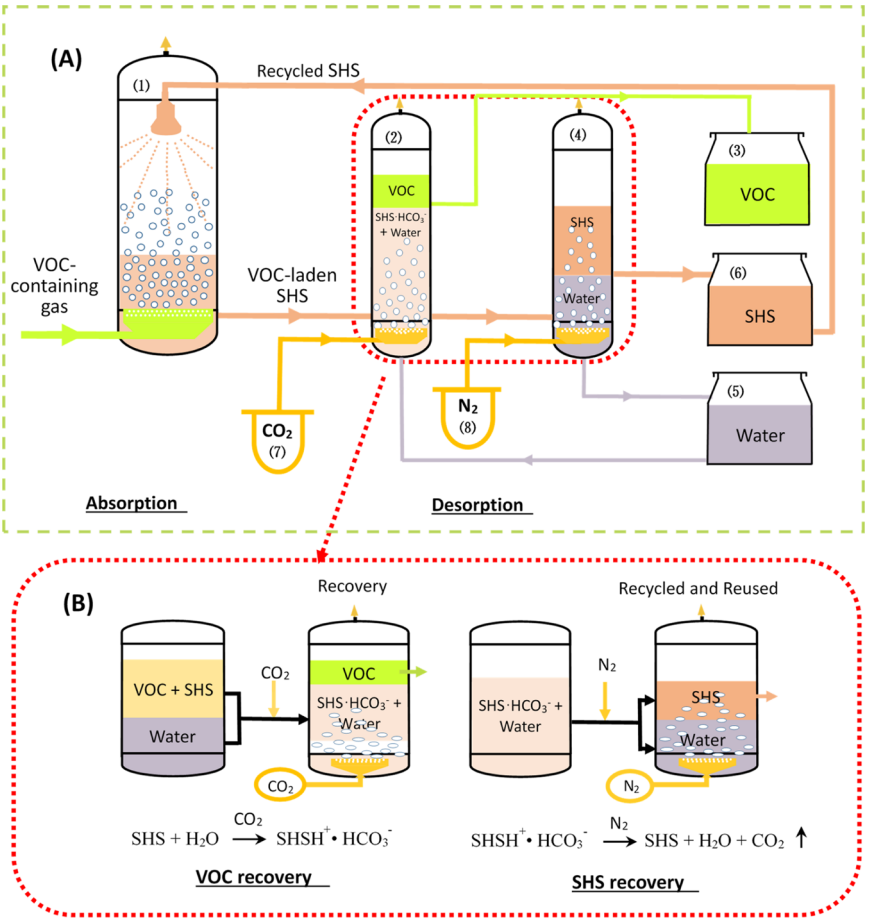

Figure 1. (A) Overall process for the absorption and desorption of VOCs using SHS as the absorbent; (B) details of the switchable desorption and regeneration steps in the process. VOC-containing gas is fed into the absorber (1) where the VOCs are absorbed by the SHS. The liquid from the absorber (1) is then sent into the desorber (2) and mixed with recovered water from tank (5). CO_2 from vessel (7) is sparged into the liquid mixture in the desorber (2) to achieve the separation of VOCs from the SHSs; then the aqueous phase solution containing SHSs and water is transported into separator (4) and is bubbled with N_2 to separate the SHS from the water. The red circle in Figure 1A is the process of desorption, the details of which are shown in Figure 1B.

alkyl-phthalates, and alkyl-adipates.[19,20] Distillation is commonly used to regenerate these absorbents.[21] However, this process yields relatively low recovery rates, consumes considerable amounts of energy, and can cause environmental damage.

In 2010, Jessop and co-workers first reported a solvent that could be removed from hydrophobic matter without distillation, which was possible because the solvent could be reversibly switched from being hydrophobic to hydrophilic.[21] They named these types of solvents switchable-hydrophilicity solvents (SHSs). An SHS is a solvent that can be made, upon application of a trigger, to reversibly switch back and forth between two states, one of which is poorly miscible with water and the other that is completely miscible with water.[21−23] Because CO_2 is nontoxic, benign, inexpensive, and easily removable, it is preferred as the trigger for the switching processes. We therefore hypothesized that SHSs could be used as absorbents to treat industrial gases containing VOCs and could be regenerated, with contaminant removal, without distillation. However, to our knowledge, use of SHS as absorbents for the removal of organic waste gases has not been reported so far. Consequently, a new method of removing VOCs was proposed based on the characteristics of SHSs. A schematic of the reversible absorption process based on SHSs is shown in Figure 1.

To test the feasibility of this new method for the removal of VOCs by SHSs, a series of experiments was conducted to examine the absorption, desorption, and recycling of SHSs for the removal of VOCs. *N*,*N*-Dimethylcyclohexylamine ($CyNMe_2$) and benzyldimethylamine (BDMA) were used as representative examples of the many known SHSs[23,25] to verify the feasibility of switchable absorption because of their commercial availability, low toxicity, and high boiling point.[22] These two SHS are water-miscible in the presence of CO_2 but largely water-immiscible in the absence of CO_2. Moreover, WO was used as a representative traditional absorbent[11] to compare with the two SHSs. Toluene was chosen as a representative VOC because it is a common toxic compound[24] with low solubility in water.[25] Although toluene might not be representative of the alkane portion of VOCs, it may be suitable as a model to test the absorption/catalytic performances of many new environmental materials.[10,26] The main goals of this study were (i) to determine the VOC absorption capacities of typical SHSs and compare them with those of more traditional absorbents; (ii) to determine Henry's law constants (E) and activity coefficients (γ) of the VOCs in the presence of SHSs, compare them with those of more

https://dx.doi.org/10.1021/acsomega.0c04443
ACS Omega 2021, 6, 253−264

traditional absorbents, and investigate the absorption kinetics of VOCs by typical SHSs; (iii) to study the desorption of VOCs from mixtures of VOCs and SHSs; and (iv) to determine the VOC absorption capacities of the regenerated SHSs.

2. MATERIALS AND METHODS

2.1. Chemicals. Chemicals, suppliers, and purities are listed in Text S1 of the Supporting Information.

2.2. Absorption. The absorption experiment equipment contained three sections: a gas mixing section to prepare the simulated waste gas, an absorption section, and an analysis section (Figure S1). The simulated gas was prepared using a bubbling method[28−30] because of its simplicity and ability to obtain a broad range of concentrations. VOC gases were prepared with N_2 as the bubbling and diluting gas in the VOC generator (100 mL), and the desired concentrations (2.6−42 g/m^3) were obtained by altering the N_2 flow rate, which was controlled by an intelligent flowmeter (DSN100CD, Dongguan De Xin Electronic Technology, Ltd. China). The experiments were performed with a total gas flow rate of 430 mL/min. Gas flow lines were constructed from Teflon tubing (3 mm OD). The VOC generator and absorber were placed in a temperature-controlled water bath to control the experimental temperature in the range of 20−55 °C. Within this temperature range, no obvious changes in the volumes of the absorption solutions were observed. Prior to the absorption experiments, the VOC gas from the generator was prepared for over 1 h until its concentration was constant.

The absorption of VOCs was performed in a glass absorber (31 mm OD × 250 mm height) with a porous glass distribution plate (8 mm OD × 250 mm length) that was immersed in the liquid absorbent to produce an even distribution of bubbles in the absorber. The absorbent (20 mL) was added to the absorber in a temperature-controlled water bath. The desired VOC/N_2 mixtures from the VOC generator were fed into the absorber at a flow rate of 430 mL/min. The VOC gas concentrations at the inlet and outlet were determined by in-line gas chromatography (GC, automatic six-way valve). The concentration of VOCs in the liquid phase,[8] $C_L(t)$, can be determined by

$$C_L(t) = \frac{Q_G}{V_L}\left(C_{G,in}t - \int C_{G,out}\,dt\right) \quad (1)$$

where Q_G (m^3/s) is the gas flow rate, V_L (mL) is the absorbent volume, $C_{G,in}$ (g/m^3) and $C_{G,out}$ (g/m^3) are the inlet and outlet concentrations of the VOC in gas flow, respectively, and t (min) is the absorption time.

2.3. Determination of Henry's Law Constants and Viscosities. In this study, headspace GC was employed to determine the Henry's law constants of toluene in different absorbents, which is an effective method for acquiring such constants according to previous studies.[26] The experiments were carried out in 40 mL headspace vials. Initially, to achieve various ratios of gas and liquid volumes, different volume standard solutions of toluene absorbents (5.1 g/L) were added into vials. The vials were placed into a shaker for 10 h to reach vapor/liquid equilibrium at a series of temperatures (three times each, in parallel). The equilibrium gas concentration of toluene was determined by GC (GC522, Shanghai Wu Feng) equipped with a flame ionization detector (FID). The GC column was a 3 m × 3 mm 10% OV-101 (Ouni Instrument Technology Co. Ltd., Shanghai). The GC operating conditions are as follows: the column, injector, and detector temperatures were set at 180, 200, and 230 °C, respectively, and the flow rates of carrier gas (N_2), hydrogen, and air were 35, 405 and 40 mL/min, respectively. The dimensionless Henry's law constants were obtained by averaging the concentrations of toluene at different ratios in the gas and liquid phases. The liquid equilibrium concentration of toluene was calculated from the conservation of mass equation

$$C_L^* = (C_S V_L - C_G^* V_G)/V_L \quad (2)$$

where C_L^* (g/m^3) and C_G^* (g/m^3) are the equilibrium concentrations of toluene in the liquid and gas in the vial, respectively, C_S (g/m^3) is the concentration of the standard solution of toluene, and V_L (mL) and V_G (mL) are the liquid and gas phase volumes, respectively.

The viscosities were determined using an NDJ Series digital viscometer (Bonsi Instrument Technology (Shanghai) Co. Ltd.). The speed was 60 rpm, and the temperature was set to 20 °C.

2.4. Determination of Mass Transfer Coefficients. The gas/liquid mass transfer of VOCs in the absorbents was carried out in a double-stirred reactor (60 mm in diameter) with four vertical baffles and two stirring blades, and the area of gas/liquid mass transfer was 2.64 × 10^{-3} m^2 (Figure S2 in the Supporting Information). The double-stirred reactor had a gas/liquid interface that was planar to a close approximation, which is an effective method for the determination of mass transfer coefficients for pollutants in absorbents at a gas/liquid interface.[33,34] The experimental setup included three sections, an organic gas generation system to prepare the simulated waste gas, a double-stirred absorption section, and an analysis system. The preparation method of the simulated gas was similar to the absorption experiments. Prior to each run, an external reactor jacket was used to maintain the desired temperature by circulating a constant temperature fluid from a temperature-controlled water bath. The liquid and gas stirring speeds were 130 and 250 rpm, respectively. The VOC vapor (15.73 g/m^3) was carried by 150 mL/min of N_2 through the reactor at different temperatures. The total pressure was set to 1 atm, and the inlet and outlet gas pressures were measured using a U-type pressure gauge. After 30 min, the absorbent was added to the rector, and the volume of the absorbent was maintained at 230 mL. The VOC concentrations in the inlet and outlet gas were analyzed using a GC−FID analyzer (automatic six-way valve).

2.5. Desorption. *2.5.1. Desorption of VOC from SHS by Bubbling CO_2.* Pure water (10 mL) and standard solutions of toluene in $CyNMe_2$ (10 mL) were placed in a graduated cylinder, which was capped with a septum. A porous glass distribution plate (3 mm OD × 300 mm length) was inserted into the bottom of the aqueous phase. Additionally, a small needle was inserted into the septum to allow the gases to escape. Various constant CO_2 flow rates were used. CO_2 was bubbled into the mixture until the volume of the upper phase was approximately constant. The desired temperature (20−55 °C) was maintained during the experiments, and the effects of temperatures on the volume changes of desorption systems can be neglected. A 1 μL sample of the toluene that separated from the mixtures was inserted into a headspace vial (40 mL, three times in parallel). After 20 min, a 0.5 mL headspace sample was removed from the vial and injected into the GC−FID with a gas-tight syringe.

https://dx.doi.org/10.1021/acsomega.0c04443
ACS Omega 2021, 6, 253−264

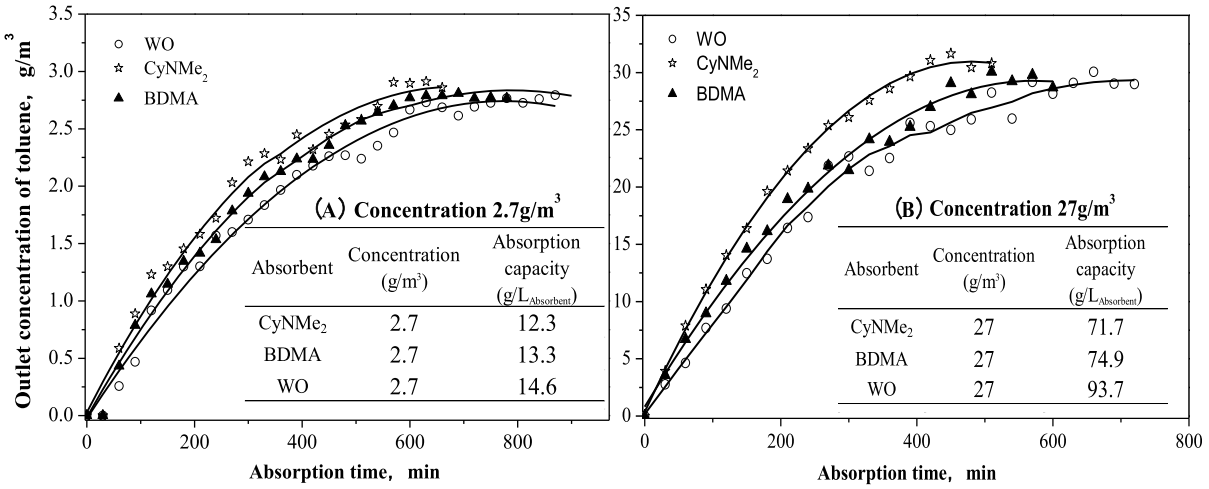

Figure 2. Comparison of toluene absorption of SHSs with common absorbents. 430 mL/min N_2 carried 2.7 g/m^3 (A) and 27 g/m^3 (B) of toluene into 20 mL of absorbent at 25 °C.

The desorption efficiency ($D_{toluene}$) of toluene was calculated as the amount of toluene collected in the upper layer divided by the total amount of toluene, which was calculated using the concentration and volume of the standard solution. In the desorption studies, the recovery of toluene was measured until the upper mixture volumes were nearly constant. The equation of the desorption efficiency of toluene in the mixture was defined as follows

$$D_{toluene} = \frac{C_G \times V_{GS} \times (V_{HV}/V_{GS}) \times (V_{upper}/V_{LS})}{C_S V_S} \times 100\% \quad (3)$$

where C_G (g/m^3) and C_S (g/m^3) are the concentrations of the headspace sample and standard solution of toluene, respectively; V_{GS} (mL), V_{HV} (mL), and V_{LS} (mL) are the volumes of the headspace sample (0.5 mL), headspace vial (40 mL), and toluene that separated from the mixtures and was inserted into a headspace vial (1 μL), respectively.

Molecular dynamics (MD) simulation was used to study the desorption process of toluene from SHSs. The simulated model was constructed by placing $CyNMe_2H^+$/toluene mixture on a water slab to form oil/water interfaces, which represents the state of $CyNMe_2$/toluene system after CO_2 was introduced. The simulations were performed using Gromacs package[35] with the GROMOS force field.[36] The configurations from the MD results were calculated by quantum mechanics (QM), and the intermolecular configurations were optimized using density functional theory at the B3LYP/6-31g* level with Gaussian 16 package.[37] Weak interaction analysis for the optimized configurations was performed using Multiwfn software.[38] The reduced density gradient was plotted against the electron density $\rho(r)$, and the gradient isosurfaces were visualized using VMD software.[39]

2.5.2. Recovery of SHS from Mixtures by Bubbling N_2. We also performed experiments to explore the separation of $CyNMe_2$ from the water phase. Mixtures (20 mL) of $CyNMe_2$ (10 mL) and pure water (10 mL) were placed in a graduated burette, which was capped with a septum. A porous glass gas distribution tube (3 mm OD × 300 mm length) was inserted into the bottom of the aqueous phase. Additionally, a small needle was inserted into the reaction tubes to allow the gases to escape. Prior to each run, a cooling jacket was fit to the top of the burette to condense steam and decrease the volume losses. Initially, a single-phase mixture of $CyNMe_2$ and pure water was obtained by bubbling CO_2 (30 mL/min, 60 min), as previously reported by Jessop et al.[21] To achieve the separation of $CyNMe_2$ from the mixture, various constant N_2 flow rates were used for the experiments (measured with a DSN500CD intelligent flow meter). N_2 was bubbled through the mixture until the volume of the upper phase was approximately constant. The temperatures (25−60 °C) were controlled for all experiments. No obvious effect of temperature was observed on the volume of the carbonated $CyNMe_2$ solutions. The equation for the recovery efficiency of $CyNMe_2$ from the water phase was defined as follows

$$R_{CyNMe_2} = \frac{V_{upper}}{V_{CyNMe_2}} \times 100\% \quad (4)$$

where V_{upper} (mL) and V_{CyNMe_2} (mL) are the volume of $CyNMe_2$ in the upper phase and the initial volume of $CyNMe_2$ (10 mL).

2.6. Recycling of SHS. $CyNMe_2$ recovered as described in Section 2.5 was used to conduct recycling experiments. In the recycling experiments, the preparation method of the simulated gas and the experimental processes were the same as described in Sections 2.3 and 2.5. Because some $CyNMe_2$ was lost during each absorption and desorption process, fresh makeup $CyNMe_2$ was added to the absorber to maintain a constant volume (20 mL) of $CyNMe_2$ after the first cyclic absorption experiment. The experiments were carried out in a 25 °C water bath, and the inlet concentration of toluene was 27 mg/L.

3. RESULTS AND DISCUSSION

3.1. Absorption Performance of SHSs toward Toluene. Figure 2 shows the gas concentration of toluene at the outlet of the absorber in the presence of different absorbents. Under a relatively low inlet concentration of toluene (2.7 g/m^3), the saturated absorption capacities of toluene in the presence of $CyNMe_2$, BDMA, and WO were determined to be 12.3, 13.3, and 14.6 g/L, respectively. The absorption capacities of toluene in the SHSs were comparable to that in WO. When nitrogen containing a high concentration of toluene was bubbled through $CyNMe_2$, BDMA, and WO,

https://dx.doi.org/10.1021/acsomega.0c04443
ACS Omega 2021, 6, 253−264

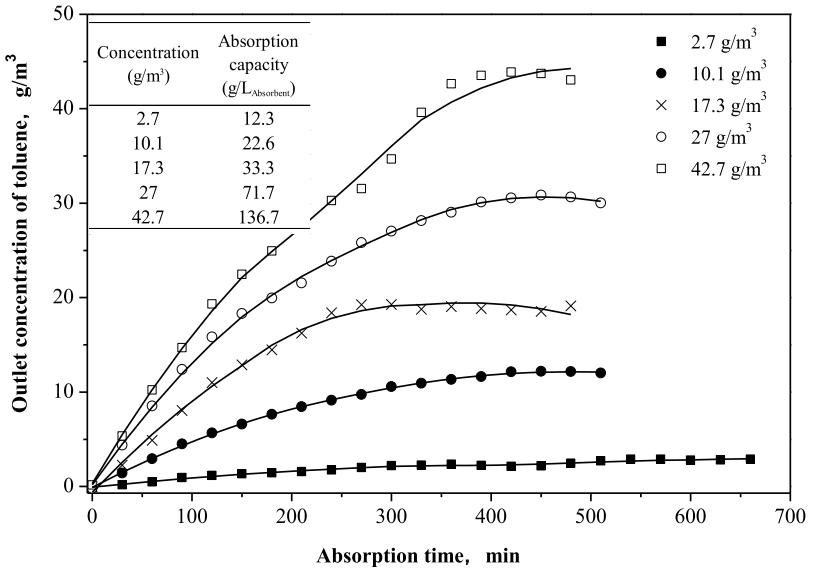

Figure 3. Effects of inlet toluene concentration on absorption capacities. 430 mL/min N_2 carried various concentrations of toluene into 20 mL of $CyNMe_2$ at 25 °C.

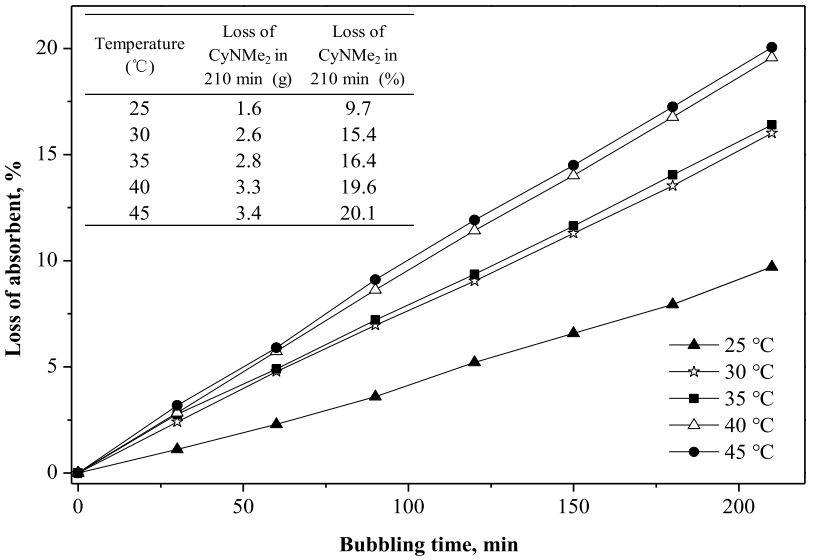

Figure 4. Effect of temperature on the loss of absorbent. 430 mL/min N_2 was bubbled into 20 mL $CyNMe_2$.

the saturated absorption capacities of toluene in $CyNMe_2$, BDMA, and WO were determined to be 71.7, 74.9, and 93.7 g/L, respectively, indicating that the absorption capacities of toluene in SHSs are slightly lower than those in WO. These results also indicate that at a relatively high toluene concentration (27 g/m^3), WO displayed a good toluene absorption capacity, 25.1 and 30.7% greater than those of BDMA and $CyNMe_2$, respectively. Nevertheless, the recycling of WO may be an issue because it does not possess switching properties like SHSs that can be separated from toluene and recycled without distillation by a simple process of bubbling CO_2/air to alter the hydrophilicity/hydrophobicity of SHSs.[21] Considering that advantage, the SHSs may be a better choice for the absorption of toluene at its typical initial concentrations.

To explore the effects of operating conditions on the toluene absorption capacity, $CyNMe_2$ was used as a representative SHS because of its comparable absorption capacity with BDMA (Figure 2) and lower toxicity than BDMA.[24] As the inlet gas toluene concentration was increased from 2.7 to 42.7 g/m^3, the absorption capacity of $CyNMe_2$ for toluene increased dramatically, ranging from 12.3 to 136.7 $g/L_{absorbent}$, respectively (Figure 3). Thus, it can be inferred that the absorption capacity of $CyNMe_2$ was enhanced by the relatively high inlet toluene gas concentrations.

As shown in Figure S3, the outlet gas concentration of toluene increased as the temperature was increased from 25 to 45 °C, indicating that the absorption capacity of $CyNMe_2$ decreased at a high absorption temperature. For example, at a low absorption temperature (25 °C), the time required to reach absorption saturation was more than 550 min at C_{in} = 2.7 g/m^3 and the absorption capacity of $CyNMe_2$ was 12.3 g/L, while at a higher temperature (45 °C), the time to saturation was less than 150 min and the absorption capacity significantly decreased to 2.4 g/L. The thermodynamic parameter Gibbs

https://dx.doi.org/10.1021/acsomega.0c04443
ACS Omega 2021, 6, 253−264

Table 1. Henry's Law Constants for Different Solute/Absorbent Systems

absorbent	temperature (°C)	$H \times 10^{-4}$ (dimensionless)	$H_C \times 10^{-3}$ (atm·L/mol)	$E \times 10^{-2}$ (atm)
$CyNMe_2$	25	2.12 ± 0.06	5.18 ± 0.14	2.86 ± 0.10
	30	3.10 ± 0.02	7.70 ± 0.51	4.22 ± 0.03
	35	5.27 ± 0.22	13.3 ± 0.54	7.28 ± 0.30
	40	7.46 ± 0.18	19.1 ± 0.47	10.0 ± 0.27
	45	10.1 ± 0.08	26.3 ± 0.21	13.7 ± 0.01
BDMA	25	2.67 ± 0.14	6.52 ± 0.34	3.64 ± 0.20
	30	5.61 ± 0.36	13.9 ± 0.89	7.53 ± 0.53
	35	8.47 ± 0.12	21.4 ± 0.31	11.3 ± 0.20
	40	13.3 ± 0.35	34.1 ± 0.89	17.7 ± 0.59
	45	20.7 ± 0.22	54.0 ± 0.58	28.3 ± 0.28
WO	25	2.43 ± 0.10	5.94 ± 0.25	3.02 ± 0.14
	30	4.01 ± 0.01	9.96 ± 0.02	5.09 ± 0.03
	35	7.00 ± 0.15	17.7 ± 0.38	8.92 ± 0.19
	40	10.7 ± 0.29	27.5 ± 0.76	13.5 ± 0.37
	45	16.0 ± 0.29	41.7 ± 0.75	22.2 ± 0.61

free-energy change (ΔG) was calculated to explore the absorption process of $CyNMe_2$ by the following equations

$$\ln K_d = -\frac{\Delta H}{RT} + \frac{\Delta S}{R} \quad (5)$$

$$\Delta G = \Delta H - T\Delta S \quad (6)$$

where K_d (C_L/C_G) is the distribution coefficient of toluene in liquid phase and gas phase, ΔH and ΔS are the enthalpy and entropy changes of absorption process, respectively, and R is the universal gas constant (8.314 J/mol/K). As indicated by Table S1, the values of ΔG in the temperature range 25−45 °C are negative, indicating that the adsorption is thermodynamically spontaneous. However, lower temperatures are beneficial for absorption because of the more negative ΔG values. These results indicate that the absorption capacity of $CyNMe_2$ was suppressed at higher absorption temperatures, suggesting that higher temperatures are unfavorable for absorption.

Loss of some of $CyNMe_2$ in the absorption process may occur due to evaporation and bubbling at various temperatures. Thus, the loss of $CyNMe_2$ in the absorption process of toluene was investigated. As shown in Figure 4, as the temperature was increased from 25 to 45 °C, the loss of $CyNMe_2$ increased from 1.6 to 3.4 g, accounting for 9.7 and 20.1%, respectively. These results indicated that a relatively high temperature condition facilitated the loss of $CyNMe_2$ in the absorption process. Thus, to maintain the absorption efficiency and reduce the loss of $CyNMe_2$, some measures should be taken, such as condensation, increasing the height of the absorption device, or selecting a less volatile SHS.

3.2. Henry's Law Constants of Toluene in SHSs and a Conventional Absorbent. According to previous studies, the values of the Henry's law constant reflect the relative VOC absorption performances of the absorbents.[31,32] Therefore, to explore the specific absorption processes, vapor/liquid equilibrium experiments (the measurement of Henry's law constant) of the absorption system were performed. Table 1 lists the values of the Henry's law constants determined at different temperatures. As indicated by Table 1, the Henry's law constants for toluene in the three absorbents were significantly influenced by the temperature. The temperature dependence of the Henry's law constant can be described by the van't Hoff equation[40]

$$\ln H = A - B/T \quad (7)$$

where the constants A and B are determined by regression analysis. The linear relationships between ln H and $1/T$ for toluene in various absorbents are shown in Figure S4. Linear relationships between ln H and $1/T$ were observed ($R^2 > 0.98$, $p < 0.05$) for the different absorption systems, suggesting that the van't Hoff equation fit the data well, and the values of A and B obtained from the regression are summarized in Table S2.

The data in Table 1 show that under different temperatures, the values of Henry's law constants for toluene in these two SHSs are slightly lower than those for toluene in WO. Moreover, the Henry's law constants in the SHSs at 25 °C were also low compared to most traditional absorbents (phthalates, polyethylene, silicon oil, and polyethylene glycol) as indicated by Table S3. This may partly explain the high absorption capacity of the SHSs relative to these many common absorbents (Table S3). To further understand the high absorption capacity of the two SHSs, we compared the values of the activity coefficient (γ) with those of common absorbents (Table S3), where the values of γ for the absorption systems were obtained by eq S7 (Text S2.1). According to previous studies, activity coefficient (γ) is a characteristic thermodynamic equilibrium parameter that reflects the interaction between toluene and the absorbent. As listed in Table S3, a γ value of an absorbent lower than unity corresponds to a more favorable thermodynamic equilibrium,[8] which indicates that the absorbents have greater trapping capacities (Text S2.2), and thus the SHSs have greater absorption capacities. In addition, the lower viscosities (η) of the SHSs compared to other absorbents promote absorption in the SHSs by enhancing the gas/liquid mass transfer rate. From these observations, it can be concluded that the values of Henry's law constants, activity coefficients, and viscosities determine the absorption capacity of SHSs for toluene.

3.3. Mass Transfer Characteristics of Absorption Process. A double-stirred reactor was used to determine the liquid phase (K_L) and gas phase (K_G) mass transfer coefficients of the SHS absorption systems for toluene. The values of K_L and K_G at 30 °C were determined to be 3.51×10^{-6} m/s and 1.85×10^{-4} mol/(m²·s·atm) using eqs S15 and S20 (Text S2.3), respectively. Therefore, combining these with the Henry's law constant, the liquid film resistance, and the gas film resistance, one can calculate H_C/K_L (2.19 m²·s·atm/mol) and $1/K_G$ (5.41×10^3 m²·s·atm/mol), revealing that $1/K_G \gg$

https://dx.doi.org/10.1021/acsomega.0c04443
ACS Omega 2021, 6, 253−264

H_C/K_L. Thus, the gas film resistance controls the absorption process of toluene in SHSs. For physical absorption, the control of the gas and/or liquid film can be estimated by an empirical formula.[41] When $\rho_s H_C/M_s P > 0.2$, the process is controlled by the liquid film, and when $\rho_s H_C/M_s P < 5 \times 10^{-4}$, the process is controlled by the gas film. In these equations, ρ_s (kg/m^3) is the density of soluble gases at the actual operating temperature, M_s (g/mol) is the toluene gas molecular weight, and P (kPa) is the total pressure of the gas phase. The calculated results, $\rho_s H_C/M_s P = 3.097 \times 10^{-4}$ (and therefore $<5 \times 10^{-4}$), indicates that the mass transfer resistance mainly exists in the gas film, which controls the entire absorption process. This result is consistent with the experimental results, confirming that the absorption process was dominated by gas film resistance.

As the temperature was an important factor affecting the absorption process, its effect on mass transfer was also investigated (Table 2). The gas- and liquid-phase mass transfer coefficients decreased with increasing absorption temperature. The dependence of the mass transfer coefficient on the temperature was determined by a linear regression using the data shown in Table 2. The correlation coefficient test showed that the logarithm of mass transfer coefficient (ln K_L and ln K_G) and $1/T$ have a linear relationship ($R^2 = 0.99$, $p < 0.05$). Thus, the influence of the absorption temperature on the gas- and liquid-phase mass transfer coefficients can be described by the following equations at constant pressure.

Table 2. Gas- and Liquid-Phase Mass Transfer Coefficients at Various Temperatures

temperature (°C)	$K_L \times 10^{-6}$ (m/s)	$K_G \times 10^{-6}$ (mol/(m^2·s·kPa))
25	3.64	1.92
30	3.51	1.85
35	3.31	1.74
40	3.16	1.66
45	2.97	1.56

$$K_L = -3 \times 10^{-8} T + 5 \times 10^{-6} \quad (8)$$

$$K_G = -2 \times 10^{-8} T + 7 \times 10^{-6} \quad (9)$$

3.4. Separation of VOCs and Recovery of SHS. It was reported previously that SHSs can be reversibly switched from being hydrophobic to hydrophilic by bubbling CO_2 through the solvent. To test whether the mixture of SHS and VOC can be efficiently separated, a switching experiment with CO_2 as a trigger was performed. As shown schematically in Figure 1B, the mixture of $CyNMe_2$ with toluene was separated upon mixing with carbonated water into two layers, where the upper layer was toluene and the lower layer was a mixture of $CyNMe_2$ (as its bicarbonate salt) and carbonated water. After removal of the toluene-rich phase, the aqueous phase (carbonated water and $CyNMe_2$) separated into two layers upon N_2 being bubbled through the mixture, where the upper layer was primarily $CyNMe_2$ while the lower layer was mostly water. The following desorption experiments were conducted to test this postulation and to optimize the operation conditions on the separation efficiency of toluene/$CyNMe_2$.

3.4.1. Desorption of Toluene from SHS by Polarity Switching of SHSs via CO_2. As listed in Table 3, there is a notable separation of $CyNMe_2$ and toluene when treated with water and CO_2, and the desorption efficiency of toluene was up to 93.7%, which verifies the feasibility of the desorption process by CO_2 control. Subsequently, we performed experiments to probe the effects of optimal conditions on the desorption efficiency of toluene in $CyNMe_2$ by varying the CO_2 flow rate, CO_2 purity, desorption temperature, volume ratio of mixtures to water, and toluene concentration. The desorption efficiencies of toluene in the mixtures versus the CO_2 flow rate for 50 min experiments are listed in Table 3. The desorption efficiencies of toluene were found to be approximately 97.7, 93.7, and 93.0% for CO_2 flow rates of 45, 30, and 15 mL/min, respectively, implying that a high CO_2 flow rate promotes the desorption of toluene in the mixed system. Although the desorption efficiency of toluene at 45 mL/min was the highest of the three flow rates, the amount of CO_2 consumption was also the highest. In addition, the desorption efficiencies of toluene with CO_2 flows at 30 and 15 mL/min were nearly equal, while the desorption time required at 15 mL/min was much longer. We concluded that the CO_2 flow rate at 30 mL/min was the most economical for the desorption processes, and hence, a 30 mL/min CO_2 flow rate was used in the subsequent experiments.

Table 3. Efficiency of Desorption of Toluene from $CyNMe_2$ Using CO_2 and Water under Different Conditions[a]

parameters	desorption of toluene (%)	bubbling time (min)	CO_2 consumption (mL)
CO_2 Flow Rate (mL/min)			
45	97.7	50	2250
30	93.7	60	1800
15	93.0	115	1725
Temperature (°C)			
20	92.5	80	2400
25	93.7	60	1800
35	92.9	70	2100
45	89.3	85	1951
55	73.7	105	3150
Toluene Concentration (g/L)			
65	92.8	75	2250
130	93.7	60	1800
260	92.0	85	2550
[b]Volume Ratio (L_{mix}/L_{up})			
10:50	96.0	45	1350
10:25	93.7	50	1500
10:16.7	93.0	50	1500
10:12.5	93.9	55	1650
10:10	93.7	60	1800
CO_2 Purity (%)			
100	93.7	60	1800
90	91.5	65	1950
80	89.1	70	2100
50	80.3	80	2400
10	65.7	150	4500
5	53.2	195	5850
1	48.2	210	6300

[a]Unless otherwise stated, CO_2 (100% purity, 30 mL/min) was bubbled into the mixtures of water (10 mL) and 10 mL of standard solution containing $CyNMe_2$ and toluene (130 g/L) at 25 °C. [b]L_{mix}/L_{up} represents the volume ratio of mixed standard solution to pure water.

https://dx.doi.org/10.1021/acsomega.0c04443
ACS Omega 2021, 6, 253−264

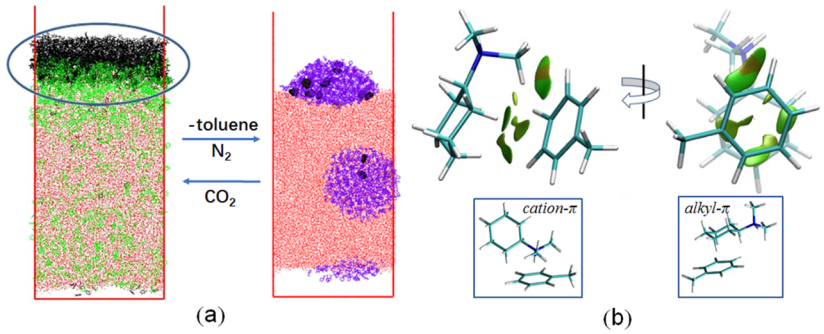

Figure 5. (a) Configuration from MD simulation. $CyNMe_2$, $CyNMe_2H^+$, toluene, and water are shown in violet, green, black, and red, respectively. (b) Gradient isosurfaces for $CyNMe_2H^+$/toluene system.

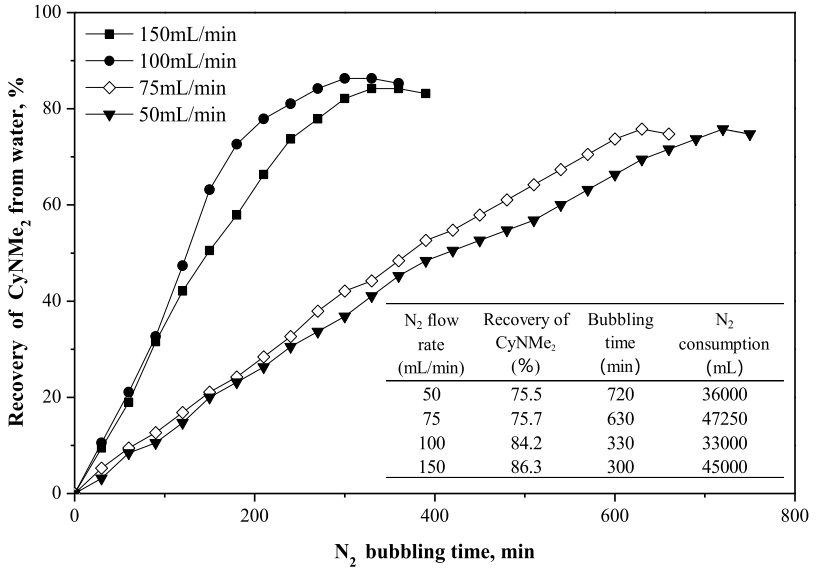

N_2 flow rate (mL/min)	Recovery of $CyNMe_2$ (%)	Bubbling time (min)	N_2 consumption (mL)
50	75.5	720	36000
75	75.7	630	47250
100	84.2	330	33000
150	86.3	300	45000

Figure 6. Comparison of the recovery of $CyNMe_2$ from carbonated water under various N_2 flow rates at 40 °C. N_2 was bubbled into a single-phase mixture of $CyNMe_2$ (10 mL) and ultrapure water (10 mL) that had been previously carbonated by bubbling of CO_2 (30 mL/min, 60 min) at 25 °C.

Table 3 also lists the effect of temperature on the desorption of toluene from $CyNMe_2$ in the range of 20−55 °C. As the temperature was increased from 20 to 55 °C, the desorption efficiency of toluene generally decreased. It is known that an increase of temperature accelerates the volatilization of toluene and leads to a decreased amount of toluene obtained, which might explain the decrease in the desorption efficiency of toluene. Moreover, amine group bicarbonates[22,27,42] are not stable and decompose easily at high temperatures, leading to reduced formation of bicarbonates,[43] poorer toluene desorption, and likely greater losses of $CyNMe_2$ to the toluene phase. Therefore, high temperatures are not conducive to the separation of toluene and $CyNMe_2$. Based on the desorption time and CO_2 consumption at different temperatures, we concluded that the temperature of 25 °C was the best for desorption, and this desorption temperature was chosen for subsequent experiments.

As can be seen in Table 3, at different initial concentrations of toluene, the desorption efficiencies of toluene were comparable. Nevertheless, at 130 g/L of toluene, the desorption process had a relatively short desorption time and low CO_2 consumption, indicating that this concentration was beneficial for the desorption of toluene from $CyNMe_2$. The effect of the proportions of the mixtures and water on the desorption process of toluene was investigated (Table 3). Upon increasing the mixture to water ratio (L_{mix}/L_{up}), the desorption efficiencies of toluene were similar, but the bubbling time and CO_2 consumption increased slightly. However, the consumption of water decreased at high mixture to water ratios (L_{mix}/L_{up}), leading to decrease of wastewater production. Thus, we concluded that a high ratio of the mixture to water is preferred for the desorption process.

We also performed experiments to examine the effects of CO_2 purity on the desorption of toluene by altering the flow proportion of N_2 and CO_2. As indicated by Table 3, the desorption efficiency of toluene from $CyNMe_2$ increased with the increase of CO_2 purity. For example, when 100% CO_2 was used, the desorption efficiency of toluene was determined to be 93.7%. However, even if the purity of CO_2 was only 1%, this was sufficient to switch the polarity of $CyNMe_2$, resulting in the desorption of toluene as high as 48.2%. This indicates that a broad spectrum of purities of CO_2 can be used as triggers to switch the polarity of $CyNMe_2$ in production and practical applications.

The desorption process mechanism for toluene from $CyNMe_2$ was probed by MD simulation. It can be seen from Figure 5a that $CyNMe_2H^+$ spontaneously entered the aqueous water phase from the organic phase, resulting in the separation

https://dx.doi.org/10.1021/acsomega.0c04443
ACS Omega 2021, 6, 253−264

of toluene and $CyNMe_2$. During this separation process, we observed that $CyNMe_2H^+$ was initially adsorbed at the oil/water interface forming an adsorption layer prior to entering into the aqueous phase, indicating that $CyNMe_2H^+$ would bind with toluene molecules through different interaction modes in this adsorption layer. Consequently, we selected the configurations from the MD results for further QM calculation. As shown in Figure 5b, noncovalent interaction occurred between $CyNMe_2H^+$ and toluene, which can be attributed to the alkyl−π interactions. Moreover, cation−π interactions formed between the $CyNMe_2H^+$ headgroup and the toluene aromatic ring also exist. However, these weak interactions cannot prevent the phase transfer of $CyNMe_2H^+$ from the organic phase to the aqueous phase because of the great hydrophilicity of the $[CyNMe_2H^+][HCO_3^-]$ salt. Therefore, $CyNMe_2$ partitions into the aqueous phase and therefore separates from toluene upon addition of CO_2 as a trigger.

3.4.2. Recovery of SHS from the Aqueous Phase upon Removal of CO_2. To recover $CyNMe_2$ from the carbonated $CyNMe_2$/water mixed solution, N_2 was bubbled through the mixture to remove CO_2 and change the hydrophilic $[CyNMe_2H^+][HCO_3^-]$ salt back into hydrophobic $CyNMe_2$, which caused the mixture to split into two liquid phases as shown in Figure 5a. As shown in Figure 6, the recovery efficiency of $CyNMe_2$ increased with the increase of N_2 flow rate from 50 to 150 mL/min. For N_2 flow rates of 100 and 150 mL/min, the recovery efficiencies of $CyNMe_2$ were comparable. Despite the somewhat short desorption time at 150 mL/min, the consumption of N_2 was considerable (Figure 6). Thus, we conclude that a N_2 flow rate of 100 mL/min was the best for the desorption process of $CyNMe_2$.

A previous study found that the separation of $CyNMe_2$ and water can also be achieved by heating.[22] We conducted experiments to investigate the effects of temperature on the desorption process. The effect of temperature on the recovery of $CyNMe_2$ in water (Figure S5) showed that the final recovery of $CyNMe_2$ at high temperatures was greater than that at low temperatures. Moreover, at high temperatures, the consumption of N_2 and the desorption time decreased dramatically. Consequently, it can be concluded that elevated temperatures significantly accelerate the desorption process, presumably because mass transfer of CO_2 out of the liquid mixture is accelerated and the rate of decomposition of amine bicarbonates increases.[22,27]

3.5. Absorption Performance of Recovered SHS toward Toluene. Recycling absorption experiments were performed to evaluate the absorption capacity of the recovered $CyNMe_2$. The absorption capacity of recovered $CyNMe_2$ slightly decreased with increasing number of cycles (Figure 7). After five absorption−desorption cycles, the absorption capacity had decreased by 10.3% compared to that of fresh $CyNMe_2$. This indicates that $CyNMe_2$ is a good reusable absorbent for the removal of VOCs. Since the $CyNMe_2$ recovered contained a certain amount of water,[44] the effect of water on the absorption capacity of $CyNMe_2$ recovered was investigated (Text S2.4). The results showed that the absorption capacity decreased with the increase of water content in $CyNMe_2$ (Figure S6). With 13.8% water content, for instance, the absorption capacity was found to be 66.2 g/$L_{Absorbent}$, which is 8% lower than that of fresh $CyNMe_2$ (71.7 g/$L_{Absorbent}$). The water content may therefore be responsible for the lower absorption capacity of recovered $CyNMe_2$ compared to fresh $CyNMe_2$.

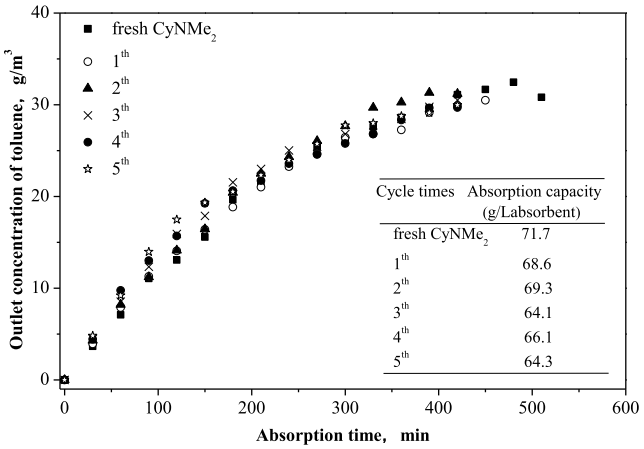

Figure 7. Effect of multiple cycles of $CyNMe_2$ on its absorption capacity for toluene at 25 °C. 430 mL/min N_2 carried 27 g/m^3 toluene absorbed by 20 mL of $CyNMe_2$ that was recovered using water, CO_2 (30 mL/min, 25 °C), and N_2 (100 mL/min, 60 °C).

The amount of water in $CyNMe_2$ carried into each cycle is controlled by the solubility limit of water at the temperature of the decarbonation step of the preceding cycle. For this reason, the water content will level out at a constant value after a few cycles rather than continue to climb. The water content can be reduced, if needed, by raising the temperature of the decarbonation step or by pretreating the wet (i.e., water-containing) recycled $CyNMe_2$ with CO_2 before use in the next cycle in order to trigger a separation of the water from the bulk of the amine.

If wet $CyNMe_2$ is exposed to a waste gas stream that contains CO_2, then much of the water in the amine is expelled from the organic liquid phase. This was demonstrated by bubbling 10 wt % CO_2 in N_2 gas mixture through a solution of 8.1 wt % water in $CyNMe_2$. A small aqueous phase, about 10% of the total liquid volume, separated from the organic phase and could be easily decanted.

The longevity of the amine is important to consider before commercial application of this technology. Decomposition should be avoided not only because of the loss of absorbent but also because the secondary amines that result from decomposition may convert to carcinogenic nitrosamines. In CO_2-capture processes, for example, the chemical decomposition of the amine is a significant problem. The amines used in such processes are ethanolamines, which typically decompose by loss of acetaldehyde (eq 10).

$$Me_2NCH_2CH_2OH \rightarrow Me_2NH + CH_3CHO \quad (10)$$

However, $CyNMe_2$ is not an ethanolamine and is therefore incapable of decomposing in this way. Additionally, the temperatures used in the toluene absorption process are significantly lower than those used in the regeneration stage of CO_2 capture processes. For both reasons, the rate of decomposition of $CyNMe_2$ should be significantly lower than that observed in CO_2-capture processes.

3.6. Engineering Implications. This study found that the SHS $CyNMe_2$ exhibited an excellent absorption performance for toluene compared to many common organic absorbents, and $CyNMe_2$ can be regenerated by bubbling CO_2 to alter the polarity of the SHS. It was reported that an organic absorbent should have the following properties to be attractive for an industrial process:[10,24] (i) a high absorption capacity, (ii) a low

https://dx.doi.org/10.1021/acsomega.0c04443
ACS Omega 2021, 6, 253−264

viscosity and a high diffusion coefficient, (iii) a low vapor pressure to reduce the loss of absorbent by stripping and to prevent possible air pollution, (iv) no toxicity or fire or explosion risks, and (v) a low cost. As indicated by Table S3, $CyNMe_2$ is less viscous than traditional absorbents, which is indicative of good diffusion ability. For the vapor pressure, Vanderveen et al.[24] reported that most SHS are less volatile than the two common VOCs, toluene and hexane, which may reduce the risk of worker exposure even if the acute toxicity (oral, rat) is greater than that of toluene and hexane. In addition, $CyNMe_2$ has a significantly higher flash point (43 °C) than toluene (4 °C) and hexane (−22 °C), indicating that the SHS is much safer than the two solvents. As for the cost of $CyNMe_2$, its price per kilogram (¥882) is comparable to or higher than many common absorbents according to the quoted price from J&K Scientific (https://www.jkchemical.com/CH/Index.html). For example, the price per kilogram of $CyNMe_2$ is slightly lower than those of diisodecyl phthalate (¥990) and silicone oil (¥984) and is higher than those of WO (¥30), di(2-ethylhexyl) adipate (¥448), diisobutyl phthalate (¥448), diisobutyl phthalate (¥184), and polyethylene glycol 400/300 (¥483/580). Based on these discussions, $CyNMe_2$ may be an alternative to common absorbents for organic waste gas. Other inexpensive SHSs exist, having even higher flash points and lower toxicity than $CyNMe_2$. They have not yet been evaluated for this application, but such screening of a range of SHS would be an important step before application of this technology.

In engineering practice, the cost for absorption of organic waste gas includes the costs of the absorbents themselves, the absorption process, and the process for the separation of the absorbents from the absorbed VOCs. In a comparison of traditional absorbents versus SHSs, the key difference is the process for separating the absorbents from the captured VOCs. In the case of traditional absorbents, the separation of absorbents is typically realized by distillation of the monophasic mixture of absorbents and VOCs. This distillation process is energy intensive and may lead to the release of volatile compounds into environment, resulting in secondary pollution. However, for the SHSs, the mixture of absorbents with VOCs can be separated by simply bubbling CO_2 at ambient temperature in the presence of water (Figure 1B). All things taken together, despite the relatively high cost of the SHSs, the SHS-based absorption process may be preferable considering the simple absorbent separation processes and the relatively low pollutant release. Of course, to guarantee compliance with emission standards related to the release of volatile pollutants during the separation processes, it may be even better to combine the SHS-based absorption process with advanced oxidation processes (e.g., photocatalysis, catalytic oxidation, and adsorption).[45]

In industrial practice, the use of air or nitrogen may not be the preferred method of stripping the CO_2 from the carbonated water because of the cost of recovering the CO_2 from the resulting gas mixture. Steam stripping or other nondiluting methods of removing CO_2 from water would likely be preferred because the recovered gas would not then be diluted by another gas, facilitating the recycling of CO_2 and thereby greatly reducing the consumption of gases.

The key advantage to this unusual absorbent is that, in contrast to most liquid absorbents for VOCs, SHS such as $CyNMe_2$ can be used as absorbents and regenerated without a distillation step, which may avoid the key disadvantages related to distillation including high energy consumption and low recovery rates. In terms of the absorption capacities of fresh and recycled $CyNMe_2$, the recovery efficiency of $CyNMe_2$, and the thermodynamic equilibrium parameters, $CyNMe_2$ proved to be a suitable absorbent for the removal of VOCs from gas. The absorption capacities of SHSs are comparable to those of many common absorbents. Many absorption conditions (e.g., initial concentration of toluene, flow rate of N_2, and temperature) can impact the absorption capacities of SHSs for VOCs. A low Henry's law constant was beneficial for the absorption of SHSs for VOCs. The desorption experiments demonstrated that in a mixture containing SHSs, VOCs, and water, VOCs were easily separated from the mixture upon bubbling of CO_2. The resulting aqueous stream containing SHSs and water could be separated upon bubbling of N_2. The SHS absorbents can be reused even after five absorption−desorption cycles. Thus, SHSs are attractive for the removal of VOCs from industrial exhaust gases.

Although some operating parameters in the industrial absorption−desorption scale, such as volumetric energy input and space velocity, have not been determined in current laboratory conditions, this study provides evidence that the developed reversible absorption process based on SHSs is feasible for removal of VOCs, and the mixture of SHSs and VOCs can be separated simply by altering the polarity of SHSs. In addition, for the high vapor pressure portion of VOCs (e.g., alkane), the reversible absorption system may be modified by screening for more suitable SHSs and/or combining with catalytic/condensed technology. Further optimization of the reversible absorption−desorption process parameters for industrial exhaust gases will be carried out in a future study.

4. CONCLUSIONS

In terms of the absorption capacities of fresh and recycled $CyNMe_2$, the recovery efficiency of $CyNMe_2$, and the thermodynamic equilibrium parameters, $CyNMe_2$ proved to be a suitable absorbent for the removal of VOCs from gas. The absorption capacities of SHSs are comparable to those of many common absorbents. Many absorption conditions (e.g., initial concentration of toluene, flow rate of N_2, and temperature) can impact the absorption capacities of SHSs for VOCs. A low Henry's law constant was beneficial for the absorption of VOCs by SHSs. The desorption experiments demonstrated that in a mixture containing SHSs, VOCs, and water, VOCs were easily separated from the mixture upon bubbling of CO_2. The resulting aqueous stream containing SHSs and water could be separated upon bubbling of N_2. The SHS absorbents can be reused even after five absorption−desorption cycles. Thus, SHSs are attractive for the removal of VOCs from industrial exhaust gases.

■ ASSOCIATED CONTENT

Supporting Information

The Supporting Information is available free of charge at https://pubs.acs.org/doi/10.1021/acsomega.0c04443.

Sources of chemicals, theory, evaluation criteria, mass transfer, K_L calculations, K_G calculations, experiments testing the effect of water, figures showing the apparatus for different experiments, a list of nomenclature and symbols, and graphs and tables presenting additional data (PDF)

https://dx.doi.org/10.1021/acsomega.0c04443
ACS Omega 2021, 6, 253−264

AUTHOR INFORMATION

Corresponding Authors

Senlin Tian − *Faculty of Environmental Science and Engineering, Kunming University of Science and Technology, Kunming, Yunnan 650500, China;* orcid.org/0000-0001-8295-0306; Phone: +86-871-65920526; Email: tiansenlin@outlook.com

Philip G. Jessop − *Department of Chemistry, Queen's University, Kingston K7L 3N6, Canada;* orcid.org/0000-0002-5323-5095; Phone: +1-613-533-6669; Email: jessop@queensu.ca

Authors

Yingjie Li − *Faculty of Environmental Science and Engineering, Kunming University of Science and Technology, Kunming, Yunnan 650500, China*

Haiyu Chang − *Faculty of Environmental Science and Engineering, Kunming University of Science and Technology, Kunming, Yunnan 650500, China*

Hui Yan − *School of Pharmacy, Liaocheng University, Liaocheng 252059, China*

Complete contact information is available at: https://pubs.acs.org/10.1021/acsomega.0c04443

Notes

The authors declare the following competing financial interest(s): PGJ is an inventor but not owner on patents covering SHS.

ACKNOWLEDGMENTS

This study was accomplished with the financial support of the National Natural Science Foundation of China (41761072 and 21777064) and the High-Level Talent Foundation of Kunming University of Science and Technology (1411909411). P.G.J. thanks the Natural Sciences and Engineering Research Council (RGPIN-2017-04528) and the Canada Research Chairs Program.

REFERENCES

(1) Goldstein, A. H.; Galbally, I. E. Known and unexplored organic constituents in the earth's atmosphere. *Environ. Sci. Technol.* **2007**, *41*, 1514−1521.

(2) Ng, N. L.; Kroll, J. H.; Chan, A. W. H.; Chhabra, P. S.; Flagan, R. C.; Seinfeld, J. H. Secondary organic aerosol formation from *m*-xylene, toluene, and benzene. *Atmos. Chem. Phys.* **2007**, *7*, 3909−3922.

(3) Rene, E. R.; Murthy, D. V. S.; Swaminathan, T. Performance evaluation of a compost biofilter treating toluene vapours. *Process Biochem.* **2005**, *40*, 2771−2779.

(4) Wei, W.; Wang, S.; Hao, J.; Cheng, S. Projection of anthropogenic volatile organic compounds (VOCs) emissions in China for the period 2010−2020. *Atmos. Environ.* **2011**, *45*, 6863−6871.

(5) Phillips, M.; Herrera, J.; Krishnan, S.; Zain, M.; Greenberg, J.; Cataneo, R. N. Variation in volatile organic compounds in the breath of normal humans. *J. Chromatogr. B: Biomed. Sci. Appl.* **1999**, *729*, 75−88.

(6) Fourmentin, S.; Landy, D.; Blach, P.; Piat, E.; Surpateanu, G. Cyclodextrins: a potential absorbent for VOC abatement. *Global NEST J.* **2006**, *8*, 324−329.

(7) Khan, F. I.; Ghoshal, A. K. Removal of volatile organic compounds from polluted air. *J. Loss Prev. Process Ind.* **2000**, *13*, 527−545.

(8) Liu, D. H. F.; Lipták, B. G. *Environmental Engineers' Handbook*, 2nd ed.; CRC Press: Boca Raton; 1999; pp 90−134.

(9) Moretti, E. C. *Practical Solutions for Reducing Volatile Organic Compounds and Hazardous Air Pollutants*; Center for Waste Reduction Technologies, American Institute of Chemical Engineers: New York, 2001.

(10) Heymes, F.; Manno-Demoustier, P.; Charbit, F.; Fanlo, J. L.; Moulin, P. A new efficient absorption liquid to treat exhaust air loaded with toluene. *Chem. Eng. J.* **2006**, *115*, 225−231.

(11) Pierucci, S.; Rosso, R. D.; Bombardi, D.; Concu, A.; Lugli, G. An innovative sustainable process for VOCs recovery from spray paint booths. *Energy* **2005**, *30*, 1377−1386.

(12) Poddar, T. K.; Sirkar, K. K. Henry's Law constant for selected volatile organic compounds in high-boiling oils. *J. Chem. Eng. Data* **1996**, *41*, 1329−1332.

(13) Darracq, G.; Couvert, A.; Couriol, C.; Amrane, A.; Thomas, D.; Dumont, E.; Andres, Y.; Le Cloirec, P. Silicone oil: an effective absorbent for the removal of hydrophobic volatile organic compounds. *J. Chem. Technol. Biotechnol.* **2010**, *85*, 309−313.

(14) Xia, B.; Majumdar, S.; Sirkar, K. K. Regenerative oil scrubbing of volatile organic compounds from a gas stream in hollow fiber membrane devices. *Ind. Eng. Chem. Res.* **1999**, *38*, 3462−3472.

(15) Schmidt, A.; Ulrich, M. Absorptionsmittel zur Reinigung lösemittelhaltiger Abluft. *Chem. Ing. Tech.* **1990**, *62*, 43−46.

(16) De Assuncao, J. V.; Vasconcelos, S. M. F. *Control of Toluene and Xylene by Absorption in Mineral Oil*; Air and Waste Management Association: Pittsburgh, PA (United States), 1997.

(17) Darracq, G.; Couvert, A.; Couriol, C.; Amrane, A.; Le Cloirec, P. Kinetics of toluene and sulfur compounds removal by means of an integrated process involving the coupling of absorption and biodegradation. *J. Chem. Technol. Biotechnol.* **2010**, *85*, 1156−1161.

(18) Kalina, A.; Wanko, H.; Weiss, S. Untersuchungen zum einfluss des wasserdampfs auf die absorption organischer komponenten mit hochsiedenden waschflüssigkeiten. *Chem. Tech.* **1994**, *46*, 1−6.

(19) Augusto, F.; Carasek, E.; Silva, R. G. C.; Rivellino, S. R.; Batista, A. D.; Martendal, E. New sorbents for extraction and microextraction techniques. *J. Chromatogr. A* **2010**, *1217*, 2533−2542.

(20) Heymes, F.; Manno Demoustier, P.; Charbit, F.; Louis Fanlo, J.; Moulin, P. Hydrodynamics and mass transfer in a packed column: case of toluene absorption with a viscous absorbent. *Chem. Eng. Sci.* **2006**, *61*, 5094−5106.

(21) Jessop, P. G.; Phan, L.; Carrier, A.; Robinson, S.; Dürr, C. J.; Harjani, J. R. A solvent having switchable hydrophilicity. *Green Chem.* **2010**, *12*, 809−814.

(22) Jessop, P. G.; Kozycz, L.; Rahami, Z. G.; Schoenmakers, D.; Boyd, A. R.; Wechsler, D.; Holland, A. M. Tertiary amine solvents having switchable hydrophilicity. *Green Chem.* **2011**, *13*, 619−623.

(23) Jessop, P. G.; Phan, L. N.; Carrier, A. J.; Rui, R.; Dominik, W. Switchable hydrophilicity solvents and methods of use thereof. U.S. Patent 8,900,444 B2, 2014.

(24) Vanderveen, J. R.; Durelle, J.; Jessop, P. G. Design and evaluation of switchable-hydrophilicity solvents. *Green Chem.* **2014**, *16*, 1187−1197.

(25) Durelle, J.; Vanderveen, J. R.; Quan, Y.; Chalifoux, C. B.; Kostin, J. E.; Jessop, P. G. Extending the range of switchable-hydrophilicity solvents. *Phys. Chem. Chem. Phys.* **2015**, *17*, 5308−5313.

(26) Gil, R. R.; Ruiz, B.; Lozano, M. S.; Martín, M. J.; Fuente, E. VOCs removal by adsorption onto activated carbons from biocollagenic wastes of vegetable tanning. *Chem. Eng. J.* **2014**, *245*, 80−88.

(27) Yang, Y.; Miller, D. J.; Hawthorne, S. B. Toluene solubility in water and organic partitioning from gasoline and diesel fuel into water at elevated temperatures and pressures. *J. Chem. Eng. Data* **1997**, *42*, 908−913.

(28) Gaudillat, P.; Jurin, F.; Lakard, B.; Buron, C.; Suisse, J.-M.; Bouvet, M. From the solution processing of hydrophilic molecules to polymer-phthalocyanine hybrid materials for ammonia sensing in high humidity atmospheres. *Sensors* **2014**, *14*, 13476−13495.

(29) Dunbar, A. D. F.; Richardson, T. H.; McNaughton, A. J.; Hutchinson, J.; Hunter, C. A. Investigation of free base, Mg, Sn, and

Zn substituted porphyrin LB films as gas sensors for organic analytes. *J. Phys. Chem. B* **2006**, *110*, 16646−16651.
(30) Lin, H.; Jang, M.; Suslick, K. S. Preoxidation for colorimetric sensor array detection of VOCs. *J. Am. Chem. Soc.* **2011**, *133*, 16786−16789.
(31) Kim, Y.-H.; Kim, K.-H. A simple method for the accurate determination of the Henry's law constant for highly sorptive, semivolatile organic compounds. *Anal. Bioanal. Chem.* **2016**, *408*, 775−784.
(32) Robbins, G. A.; Wang, S.; Stuart, J. D. Using the static headspace method to determine Henry's law constants. *Anal. Chem.* **2002**, *65*, 3113−3118.
(33) Jiang, L.; Tian, S.; Ning, P.; Mo, H. Solubilization absorption of toluene vapor by formation of oil-in water microemulsions with cation surfactants. *Sep. Sci. Technol.* **2010**, *45*, 508−514.
(34) Wang, J.; Lu, P.; Wang, Z.; Yang, C.; Mao, Z.-S. Numerical simulation of unsteady mass transfer by the level set method. *Chem. Eng. Sci.* **2008**, *63*, 3141−3151.
(35) Hess, B.; Kutzner, C.; van der Spoel, D.; Lindahl, E. GROMACS 4: Algorithms for highly efficient load-balanced, and scalable molecular simulation. *J. Chem. Theory Comput.* **2008**, *4*, 435−447.
(36) Oostenbrink, C.; Soares, T. A.; van der Vegt, N. F. A.; van Gunsteren, W. F. Validation of the 53A6 GROMOS force field. *Eur. Biophys. J.* **2005**, *34*, 273−284.
(37) Frisch, M. J.; Trucks, G. W.; Schlegel, H. B.; Scuseria, G. E.; Robb, M. A.; Cheeseman, J. R.; Scalmani, G.; Barone, V.; Petersson, G. A.; Nakatsuji, H.; Li, X.; Caricato, M.; Marenich, A. V.; Bloino, J.; Janesko, B. G.; Gomperts, R.; Mennucci, B.; Hratchian, H. P.; Ortiz, J. V.; Izmaylov, A. F.; Sonnenberg, J. L.; Williams-Young, D.; Ding, F.; Lipparini, F.; Egidi, F.; Goings, J.; Peng, B.; Petrone, A.; Henderson, T.; Ranasinghe, D.; Zakrzewski, V. G.; Gao, J.; Rega, N.; Zheng, G.; Liang, W.; Hada, M.; Ehara, M.; Toyota, K.; Fukuda, R.; Hasegawa, J.; Ishida, M.; Nakajima, T.; Honda, Y.; Kitao, O.; Nakai, H.; Vreven, T.; Throssell, K.; Montgomery, J. A., Jr.; Peralta, J. E.; Ogliaro, F.; Bearpark, M. J.; Heyd, J. J.; Brothers, E. N.; Kudin, K. N.; Staroverov, V. N.; Keith, T. A.; Kobayashi, R.; Normand, J.; Raghavachari, K.; Rendell, A. P.; Burant, J. C.; Iyengar, S. S.; Tomasi, J.; Cossi, M.; Millam, J. M.; Klene, M.; Adamo, C.; Cammi, R.; Ochterski, J. W.; Martin, R. L.; Morokuma, K.; Farkas, O.; Foresman, J. B.; Fox, D. J. *Gaussian 16*, Revision C.01; Gaussian, Inc.: Wallingford CT, 2016.
(38) Lu, T.; Chen, F. Multiwfn: a multifunctional wavefunction analyzer. *J. Comput. Chem.* **2012**, *33*, 580−592.
(39) Humphrey, W.; Dalke, A.; Schulten, K. VMD: Visual molecular dynamics. *J. Mol. Graphics* **1996**, *14*, 33−38.
(40) Gossett, J. M. Measurement of Henry's law constants for C1 and C2 chlorinated hydrocarbons. *Environ. Sci. Technol.* **1987**, *21*, 202−208.
(41) Tu, J. L.; Wu, Z. Q. *Absorption Operation in Chemical Industry: Engineering and Technology of Gas Absorption*; East China University of Science and Technology Press: Shanghai, 1994; pp 42−75.
(42) Jessop, P. G.; Heldebrant, D. J.; Li, X.; Eckert, C. A.; Liotta, C. L. Green chemistry: reversible nonpolar-to-polar solvent. *Nature* **2005**, *436*, 1102.
(43) Pellegrini, G.; Strube, R.; Manfrida, G. Comparative study of chemical absorbents in postcombustion CO_2 capture. *Energy* **2010**, *35*, 851−857.
(44) Stephenson, R. M. Mutual solubilities: water + cyclic amines, water + alkanolamines, and water + polyamines. *J. Chem. Eng. Data* **1993**, *38*, 634−637.
(45) Yang, C.; Miao, G.; Pi, Y.; Xia, Q.; Wu, J.; Li, Z.; Xiao, J. Abatement of various types of VOCs by adsorption/catalytic oxidation: A review. *Chem. Eng. J.* **2019**, *370*, 1128−1153.

https://dx.doi.org/10.1021/acsomega.0c04443
ACS Omega 2021, 6, 253−264